6

Characterization of Carbon from the Bark of *P. juliflora* by Plasma Synthesis

6.1. Introduction

In consideration with the superiority of biomass material highlighted in previous Chapters, carbon has been prepared from the bark of *P. juliflora* by plasma synthesis without using any of the chemicals or any pre/post-activation processes. The S-Carbon had very poor electrochemical performance and B-Carbon resulted in highly disordered graphite with better performance. The results of next attempt of carbon preparation from the bark of *P. juliflora* by plasma synthesis is referred as **PB-Carbon** throughout the discussion.

6.2. X-Ray Diffraction Analysis of PB-Carbon

The diffraction peaks observed in the PB-Carbon is, similar to that of S-Carbon, shown in Figure 35. It is fitted by Gaussian function and shows two peaks at 26.23° and 45.28° which corresponds to the (002) and (101) hkl planes respectively. The sharp and high intense peak at 26.23° reveals the higher degree of crystallization in the PB-Carbon. The intensity ratio between (002) and (101) planes are compared with previous reports described in Chapter 4.

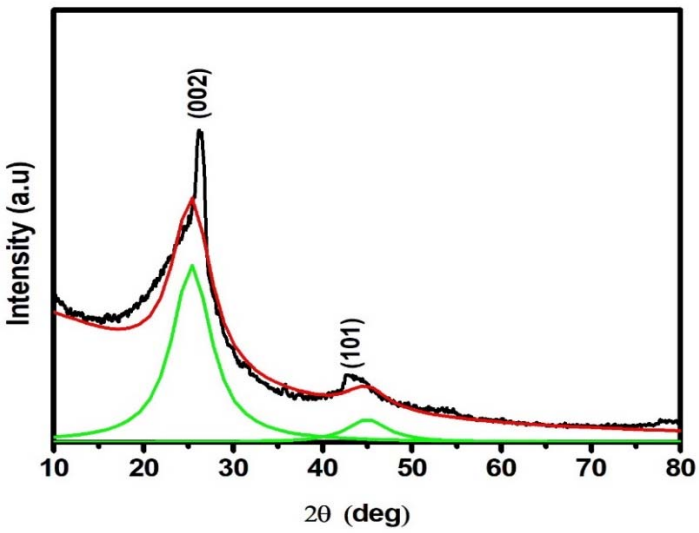

Figure 35 - X-ray Diffractogram of PB-Carbon

In the present case, the ratio is 5.5 which is higher than the reported articles and B-Carbon confirms the higher crystallinity of the sample in specific orientation along (002) plane. From XRD analysis, it concludes that there is a possibility of making graphitized carbon without activation and/or chemicals during the synthesis process.

6.3. Raman Analysis of PB-Carbon

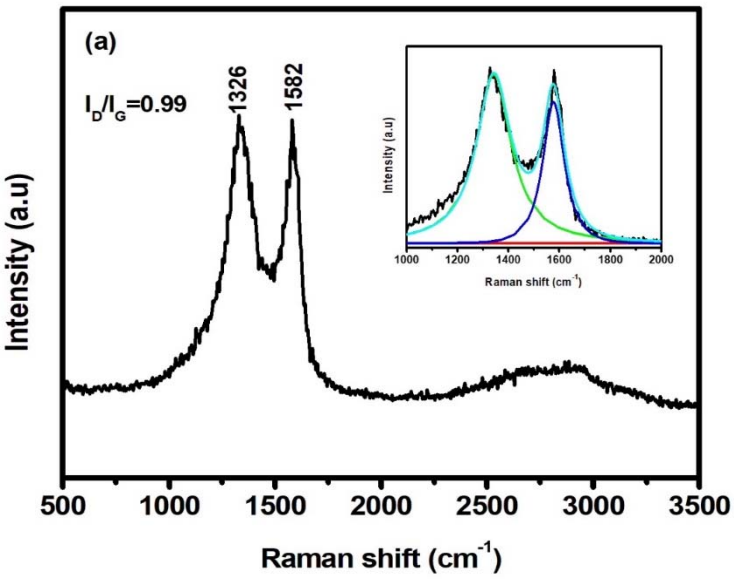

Figure 36a - Raman spectra of PB-Carbon

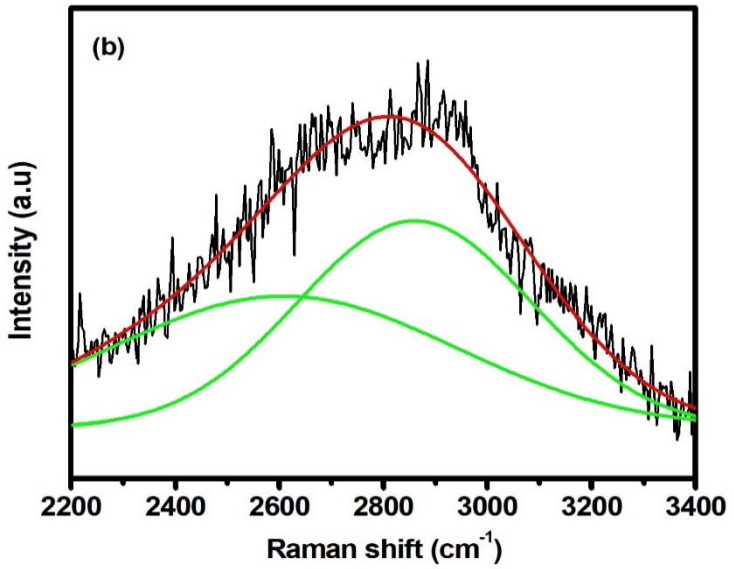

Figure 36b - Raman spectra of PB-Carbon – Deconvoluted 2D band

Raman spectrum of PB-Carbon is shown in Figure 36a. The inset shows the fitted Raman spectra of B-Carbon. It shows D and G band at 1326 cm^{-1} and 1582 cm^{-1} respectively. In PB-Carbon, compared to D band, the prominent G band is observed which indicates the high degree of graphitization in the sample. The calculated I_D/I_G ratio of PB carbon is 0.99 (I_D/I_G< 1.00) and the obtained value is lower than the B-Carbon and the already reported works [explained in Chapter 4]. It further confirms that the PB-Carbon exhibits higher graphitization degree along with lower D band freedom. Double resonance mechanism peak of D band is observed at 438 cm^{-1}. The very broad peak observed with maxima at 2834 cm^{-1} is deconvoluted using Origin software into two peaks with peak maxima at 2866 cm^{-1} (D+G band) and 2600 cm^{-1} (2D band), shown in Figure 36b. It reveals the prominent D+G band and no significant 2D band, suggesting that the prepared PB-Carbon has more graphitization than the defect sites, which could enhance the electrochemical performance.

6.4. FESEM analysis of PB-Carbon

The FESEM micrographs of the PB-Carbon at different magnifications are given in Figure 37a and 37b. The prepared PB Carbon exhibits a porous structure, which supports the electro-adsorption process for electric double layer capacitors. The physical observation of PB-Carbon show needle like structures that are seen as smooth and longer strands in low magnification micrograph. It is due the appearance of free-flowing carbon filings of prepared PB-Carbon with the dimension approximately <0.5mm. Whereas, in the case of carbon from the bark and stick of *P. juliflora* by the conventional heating method, the appearance of the prepared sample is granulated.

Hence, the different morphology i.e., fibre-like morphology shown in FESEM micrographs of PB Carbon. Further magnification to x10000 at 2 μm scale on these strands showed severe pores as seen in the Figure 37b. Further magnified FESEM image at 100 nm scale shows the diameter of pore in the range of 26 nm, as per IUPAC classification which belongs to the mesopores (2-50 nm).

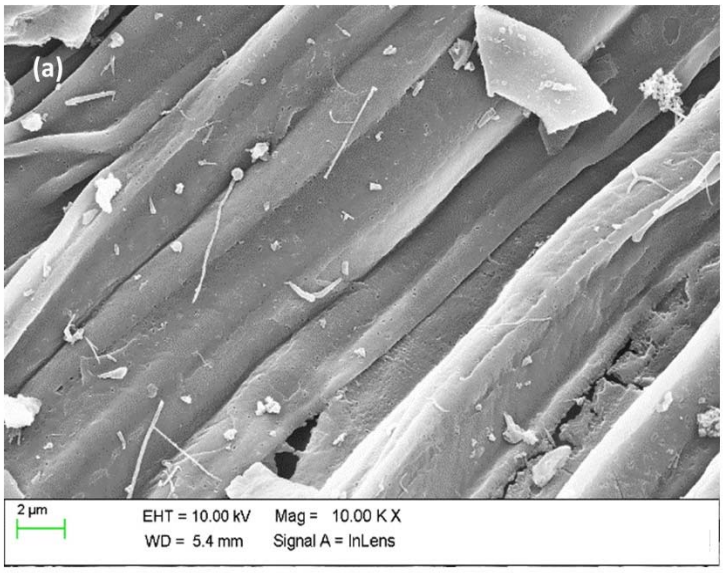

Figure 37a - FESEM micrograph of PB-Carbon at lower magnification

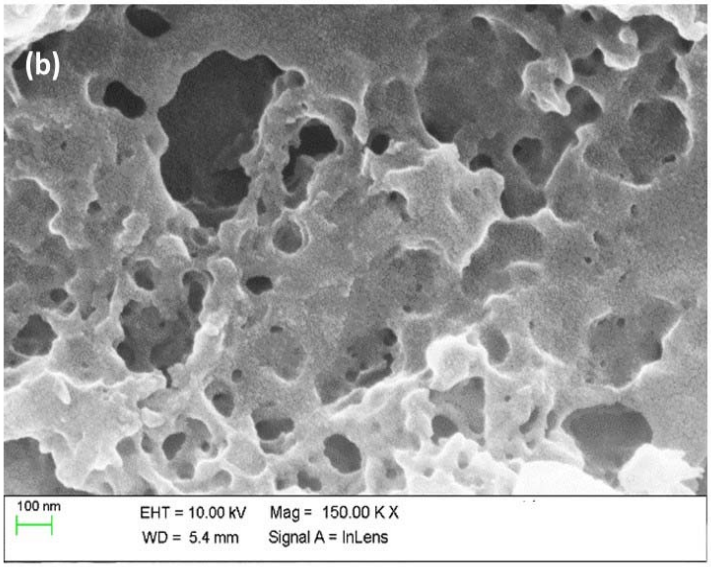

Figure 37b - FESEM micrograph of PB-Carbon at higher magnification

6.5. HRTEM analysis of PB-Carbon

HRTEM analysis of PB-Carbon is given in Figure 38. The low magnification micrograph shows graphitic texture very obviously in Figure 38a. When magnified further, graphitic formation with parallel cleavage is seen as micro crystallites very clearly that is

shown in Figure 38b. The specific area of micro crystallite is zoomed for better viewing and its corresponding FFT processed image is shown in Figure 38c. This is in good agreement with XRD and Raman results of higher crystallinity.

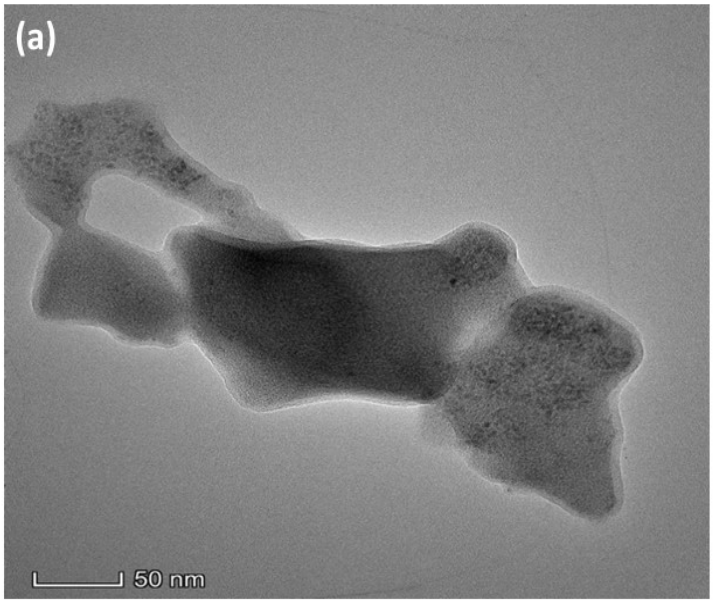

Figure 38a - HRTEM images of PB-Carbon at lower magnification

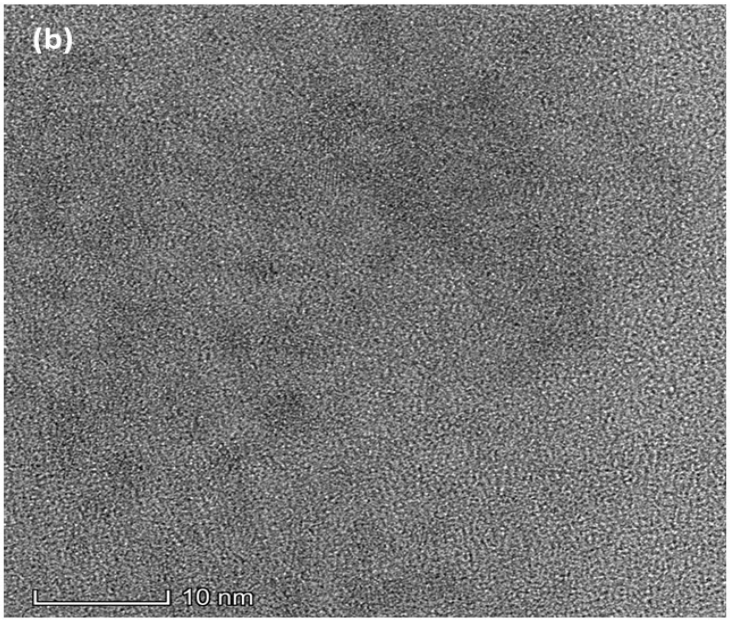

Figure 38b - HRTEM images of PB-Carbon at higher magnification

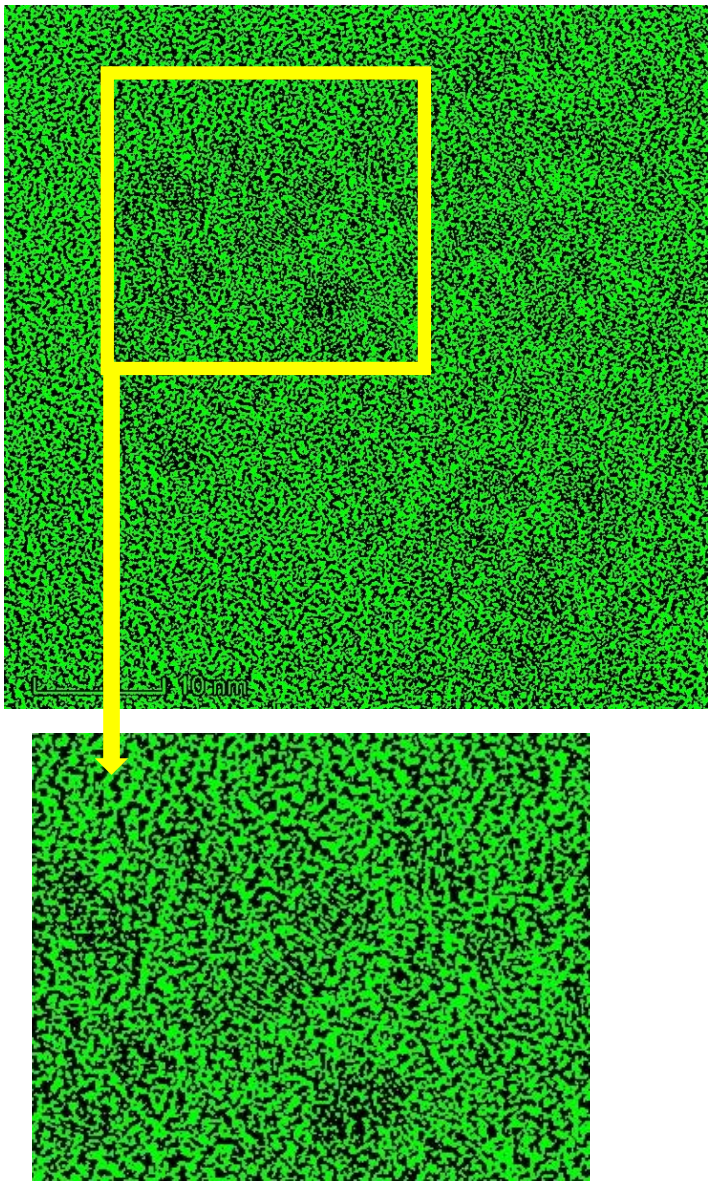

Figure 38c – FFT processed HRTEM image of PB-Carbon at higher magnification

6.6. Elemental analysis of PB-Carbon

Compositional analysis of the PB-Carbon is given in Figure 39. It has higher amount of carbon along with traces of nitrogen, sulfur and oxygen elements. Apart from the carbon content, PB-Carbon has no metal contents (Ca, K, Si). Also, carbon prepared from the bark of *P. juliflora* by conventional heating method had no metal contents which was discussed in the previous Chapter. But, the carbon prepared from the stick of

P. juliflora by the conventional method contained metal contents. The EDX of B-Carbon and PB carbon thus clarifies that there are no cationic impurities. Hence, the cationic impurities in S-Carbon should have emerged only from the stick of *Prosopis juliflora* and is not present in the Bark of the plant. The atomic weight percentage of elements in the PB-Carbon is given in Table 14. The atomic weight percentage of carbon prepared by plasma synthesis is 88.07% which is significantly higher than the reported literature on activated carbon from various biomass and the corresponding references are mentioned in Chapter 4.

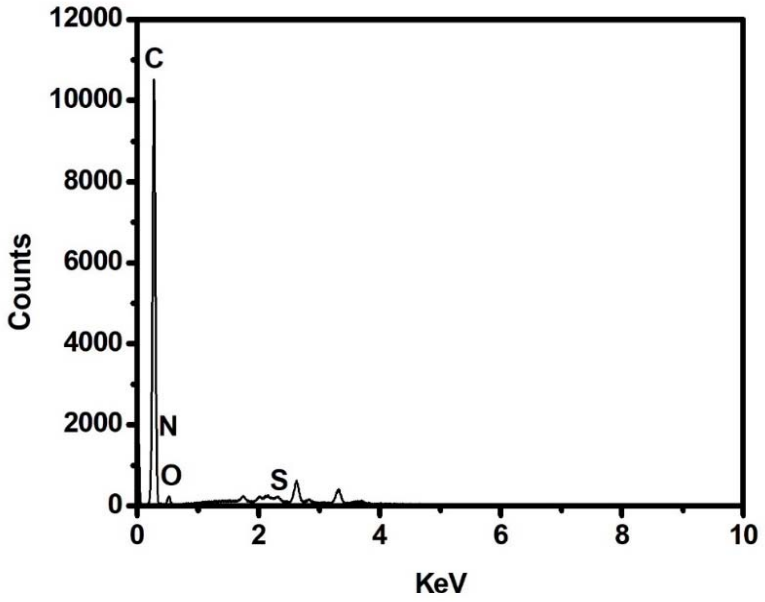

Figure 39 – EDX spectrum of PB-Carbon

Table 14 - Elemental composition of PB-Carbon

Elements	At. Wt.%
Carbon	**88.07**
Oxygen	6.11
Nitrogen	5.66
Sulfur	0.16

6.7. BET Surface Area Analysis of PB-Carbon

N_2 adsorption-desorption analysis was performed to study the porosity of the prepared material, as shown in Figure 40. As per the classification of the International Union of Pure and Applied Chemistry, the plasma carbon reveals a Type-IV isotherm. The increase in adsorption at low relative pressure suggests that the volume of the nitrogen adsorbed by the microporous range of the plasma carbon is less. The decrease in adsorption at high relative pressure shows the significant hysteresis loop, which indicates that the material possesses more mesopores compared to micropores. The size of the mesopores is subsequently larger than the size of the solvated ions (K^+ = 2.8 Å and OH^- = 1.33 Å). The amount of nitrogen adsorbed is increased when the high relative pressure >0.9, which suggests the presence of macropores in the plasma carbon. The specific surface area of the sample is observed to be S_{BET} = 38 $m^2\ g^{-1}$. From Figure 41, the observed pore volume from the Barrett, Joyner, and Halenda method for the plasma carbon is 0.032 $cm^3\ g^{-1}$ and the average pore diameter is 3.928 nm. Surface area analysis concluded that the pore diameter observed through the Brunauer, Emmett and Teller (BET) analysis, as given in Figure 41, starts from 2.18 nm, inferring that mesopores prevail in the plasma carbon.

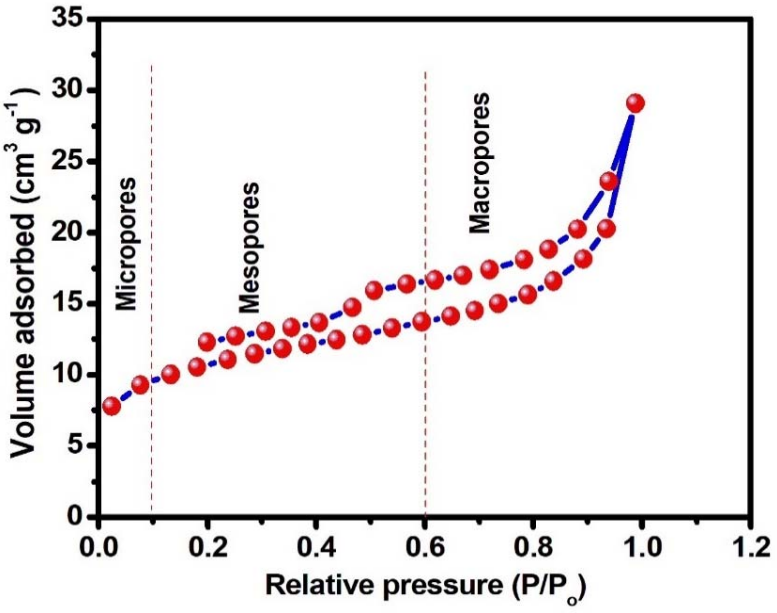

Figure 40 – BET analysis of PB-Carbon

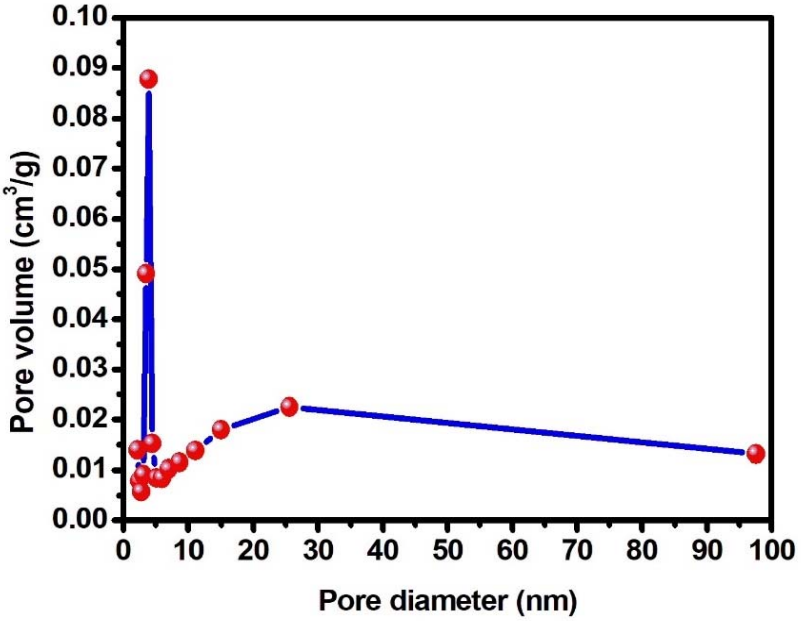

Figure 41 – Pore size distribution of PB-Carbon

Hence, the micropores (if any) present in the sample would boost the capacitance by increasing the specific surface area. In this case, it is to be noted that the performance offered would majorly be due to mesopores. It can promote the effective utilization of the pore surface and enhance the charge transfer so that it improves the electrochemical performance

6.8. Electrochemical Analysis of PB-Carbon

6.8.1. Cyclic Voltammetry Analysis of PB-Carbon

The CV analysis of PB-Carbon at various scan rates from 10 mV/s to 100 mV/s is given in Figure 42. The charge and discharge currents should be the same in an ideal supercapacitor with a constant CV potential scan rate and also the CV curve should be rectangular. In the present case, it can be seen that the prepared PB-Carbon exhibits a rectangular like profile indicating characteristic EDLCs behaviour with slight pseudocapacitive impression similar to the S-Carbon. From the obtained CV curves, the specific capacitance (Fg^{-1}) of PB-Carbon is calculated according to Equation 1 in Chapter 3. The specific capacitance values of PB-Carbon are 85, 65, 48, 40, 35, 29 Fg^{-1} at 10, 20, 40, 60, 80 and 100 mV/s respectively.

6.8.2. Galvanostatic Charge-Discharge analysis of PB-Carbon

The GCD curves of carbon prepared by plasma synthesis at various current densities from 1 Ag^{-1} to 3 Ag^{-1} are shown in Figure 43. The curves show quasi- triangular shapes which is similar to the GCD curves of S-Carbon. The specific capacitance of PB-Carbon can be calculated based on the relation (2). The specific capacitance values of the PB-Carbon are 81, 61, 42, 34 and 27 Fg^{-1} at the current densities of 1, 1.5, 2, 2.5 and 3 Ag^{-1} respectively. Figure 44 shows the change in specific capacitance with respect to current density of the PB Carbon. Comparatively, the specific capacitance value of PB-Carbon is lower than B-Carbon and previously reported articles of activated carbon from various biomass as mentioned in the Chapter 4. Due to the low specific surface area of PB-Carbon, the non-availability of active sites for electrolytic ions have resulted in low specific capacitance.

The cyclic stability of PB-Carbon has been evaluated for 500 charge/discharge cycles and shown in Figure 45. The carbon prepared from the bark of *P. juliflora* by plasma synthesis still retains 82% of its initial capacitance indicating the outstanding cyclic stability of the material. Comparatively, it is higher than B-Carbon due to less redox behaviour noted from the electrochemical performance of PB-Carbon, as seen in the CV and GCD analysis of the sample.

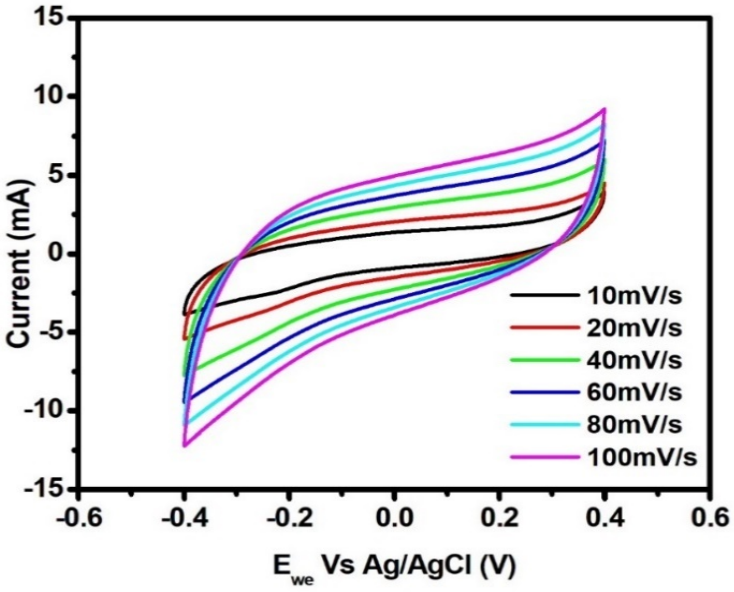

Figure 42 - Cyclic voltammogram of PB-Carbon

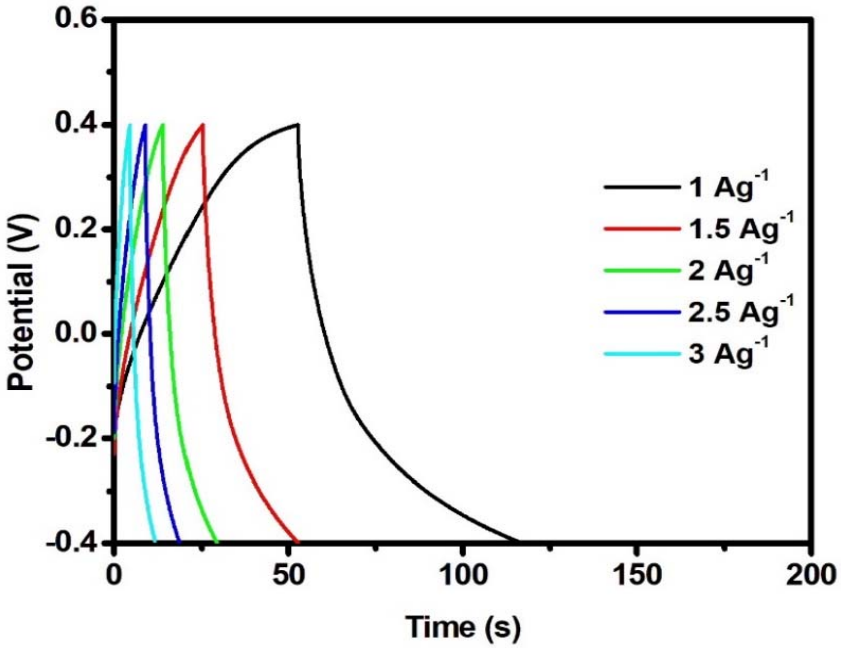

Figure 43 - Galvanostatic Charge-Discharge curves of PB-Carbon

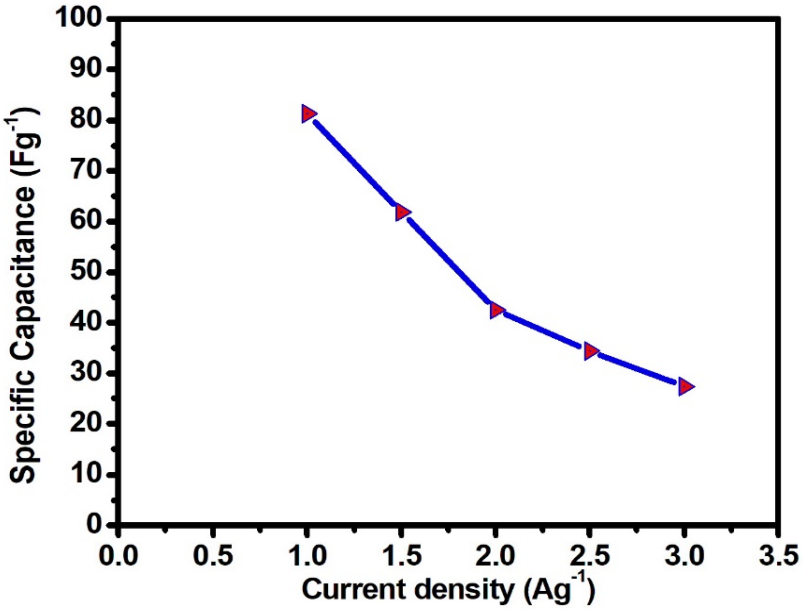

Figure 44 - Plot of current density vs specific capacitance of PB Carbon

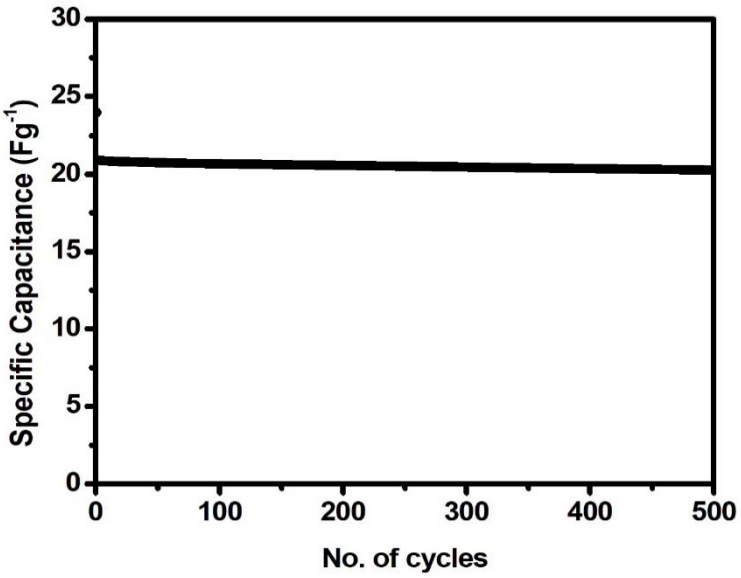

Figure 45 - Cyclic stability of PB-Carbon

6.8.3. Electrochemical Impedance Analysis of PB-Carbon

The electrochemical impedance analysis of PB-Carbon is measured in the frequency range of 100 mHz to 10 KHz in room temperature. The corresponding Nyquist plot is shown in Figure 46. The equivalent circuit of PB carbon is similar to that of S-Carbon. The fitted parameters from the equivalent circuit are shown in Table 15. Before and after cycling, the charge transfer of PB-Carbon is 3.77 Ω and 58.76 Ω. Compared to B-Carbon, PB-Carbon exhibits higher charge transfer resistance. This can be looked as a consequence formation of microcrystallites. When highly disordered graphite is observed in B-Carbon, the charge transfer resistace was low due to the increased available surface area. When microcrystallites forms, this surface area becomes lower thus increasing the charge transfer resistance. Also, after cycling the charge transfer resistance is increased which affects the cyclic stability of the sample over 500 cycles.

The electrochemical performance of PB-Carbon is lower than B-Carbon. It is due to the low specific surface area (S_{BET} = 38 m^2g^{-1}) of the sample. However, the specific capacitance of carbon from B-Carbon is more or less equal to the S-Carbon which suggests that the further optimization of plasma carbon at different plasma conditions like temperture, height of the torch from biomass, could achieve the better electrochemical performance.

It also paves the way to new opening for the preparation of electrode material without any chemical activation that could simplify the synthesis procedure facilitating the large scale production.

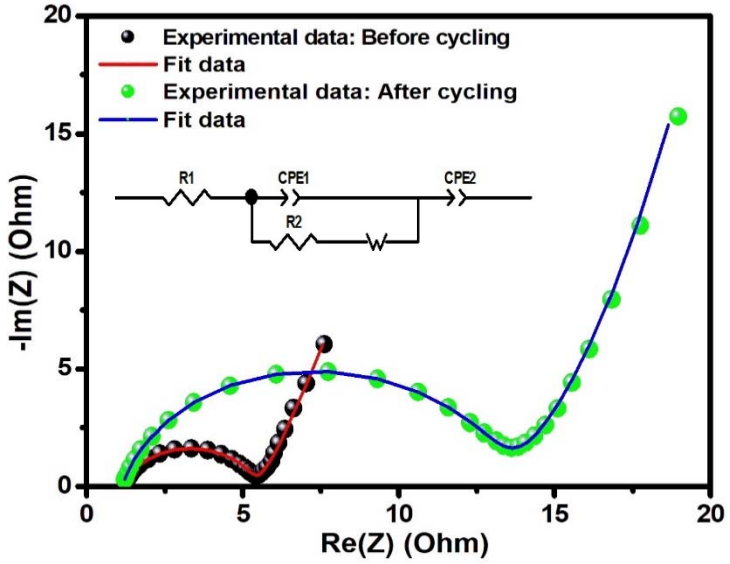

Figure 46 - Electrochemical impedance spectra of PB-Carbon before and after cycling

Table 15 - Fitted parameters of electrochemical impedance spectra of PB-Carbon

Parameters	PB-Carbon	
	Before cycling	After cycling
$R_1(\Omega)$	3.58	4.30
$R_2(\Omega)$	3.77	58.76
CPE 1	0.26×10^{-3}	0.28×10^{-3}
n1	0.79	0.78
CPE 2	0.18	0.08
n2	0.95	0.68
W	8.05	25.3

6.9. Summary

In the anodic part of the supercapacitors, S-Carbon and B-Carbon have been prepared from the stick and bark of *Prosopis juliflora* by conventional heating method. Then, high performance biomass i.e., bark of *Prosopis juliflora,* PB Carbon, has been synthesized by plasma firing without using any activating agents explored in this Chapter. A comparison of different results for all the three carbons prepared from *Prosopis juliflora* is consolidated in the Table 16. The existence of highly oriented graphitic microcrystallites are verified by high intense (002) peaks and (101) planes of XRD. The existence of D and G band in Raman analysis of all the prepared carbons and in addition D+G bands and double resonance of D bands are also observed. Generally, D band broadening is an indication of disorderliness in graphite and weak bands corresponding to D' and D" bands will be seen on highly disordered graphite.

Table 16 - Comparison of performances for all the three carbons prepared from *P. juliflora*

Performance	S-Carbon	B-Carbon	PB-Carbon
I_D/I_G ratio	0.97	**1.09**	0.99
I_{2D}/I_G ratio	0.02	**0.22**	0.06
Specific surface area (m^2g^{-1})	6.38	**703**	38
Specific capacitance (Fg^{-1})	84	**198**	81

The D band, 2D bands are highly sensitive to defects and it is compared as I_{2D}/I_G for all the three cases S- Carbon - 0.02, B-Carbon -0.22 and PB-Carbon -0.06. From these values, correlating to the specific capacitance values B -Carbon has given better performance. Also looking into the surface area obtained from BET analysis, S-Carbon 6.38 m^2g^{-1}, B-Carbon 703 m^2g^{-1} PB-Carbon 38 m^2g^{-1}. Both raman and BET converges to the fact that the extent of disordered structure in the achieve graphitization favors the electrochemical performance since the specific capacitance of B-Carbon is 198 Fg^{-1}. Hence, out of all the results B Carbon has high specific capacitance.